NanoSpec: A diffraction limited micro-spectrograph for pico- and nano-satellites.

Christopher H. Betters[*a,b], S.G. Leon-Saval[a] and J. Bland-Hawthorn[a,b]

[a]Institute for Optical Science, School of Physics, University of Sydney, Australia;
[b]Sydney Institute for Astronomy, School of Physics, University of Sydney, Australia

ABSTRACT

Here we present a novel diffraction limited spectrograph (NanoSpec) designed for integration in the 0.75kg i-INPSIRE satellite at the University of Sydney. NanoSpec is a single-mode fibre fed spectrograph operating very close to the diffraction limit over a wavelength range of 450nm to 700nm. The spectrograph is fed light via a single-mode (and thus diffraction limited) fibre pseudo-slit, allowing an extremely compact spectrograph while maintaining high performance. The current design has two configurations (for two different detectors), both achieving diffraction limited resolving powers ($\lambda/\Delta\lambda$) of 650 and 1400 respectively. The primary goal of NanoSpec is to demonstrate the potential of the PIMMS (photonic integrated multimode micro-spectrograph) type design for deployment in high altitude and space-based applications. To that end we present the optical design and laboratory based testing in preparation for a high altitude ballon launch and later on the i-INPSIRE satellite.

Keywords: instrumentation: diffraction limited; instrumentation: micro-spectrographs; high resolution; Gaussian beam; pico-satellite; Čerenkov radiation and astrophotonics

1. INTRODUCTION

NanoSpec is a diffraction limited single-mode fibre (SMF) fed spectrograph based upon the PIMMS#0 concept described by Bland-Hawthorn *el al.* in 2010.[1] The concept is inspired by the efficient multi-mode to single-mode conversion of the photonic lantern.[2–4] These allow for a spectrograph to be fed light by an array of SMF. Given the fundamental form of propagation in SMF, this is equivalent to smallest possible input slit that can be used on a spectrograph (it is diffraction limited). Consequently, the spectrograph resolving power becomes dependant purely on the dispersing element, namely the number of lines illuminated on the diffraction grating. Additionally, it allows for the an extremely compact design and reduces complexities in alignment and construction, making it suitable for use in a small satellite, such as the i-INPSIRE pico-satellite project at The University of Sydney.[5–7]

The target orbit for i-INSPIRE is a high inclination polar orbit with an altitude of ~310 km, remaining in space for 20-40 days (>320 orbits). Of particular interest, from the perspective of the NanoSpec design, is the short term effects of radiation on optical components. For example, Čerenkov light that can be generated in the optical fibre feed in periods of high radiation, such as passing through the South Atlantic anomaly (SAA).

Here we will first briefly inroduce the expected radiation environment in orbit and its implications on the spectrograph design. We then describe the design of NanoSpec, and present a brief report on the engineering version's performance. We close with a discussion of future plans and possibilities.

2. RADIATION ENVIRONMENT

The radiation environment in low earth orbit (LEO) is a combination of galactic cosmic rays, particles trapped in the Earth's magnetic field (also known as trapped radiation or the Van Allen belts) and particles generated by energetic solar events, such as flares or coronal mass injections. Trapped radiation is the dominant source of high energy particles in high inclination polar orbit planned for i-INSPIRE.[8–10]

There are two hot spots of radiation: at the poles, where electron precipitation is highest, having been funnelled to this region by the Earth's magnetic field; and at the South Atlantic anomaly, where the inner radiation belt is closest to the earths surface. It is in these regions we expect any effects of radiation to present themselves in NanoSpec and the satellite control systems.

[*]c.betters@physics.usyd.edu.au

Space Telescopes and Instrumentation 2012: Optical, Infrared, and Millimeter Wave, edited by Mark C. Clampin, Giovanni G. Fazio, Howard A. MacEwen, Jacobus M. Oschmann, Jr., Proc. of SPIE Vol. 8442, 84424B

2.1 Implications

i-INSPIRE's compact size and limited weight eliminate the possibility of any substantial radiation shielding. As a result all the components will be exposed to a relatively strong radiation environment (flux $> 10^3$ particles/s/cm^2 with an energy larger then 0.2 MeV). Besides single event upset occurrences, which can cause the computer or detector to malfunction, we are particularly interested in the possibility of Čerenkov light being generated by high energy particles in the optical fibre feed of NanoSpec. Čerenkov radiation is commonly pictured as the blue glow seen around submerged nuclear reactors, but is also central to many particle, astrophysics and space experiments.[11,12]

Čerenkov photons are generated when a charged particle passes through a material (with refractive index n) faster then the speed of light in that material (i.e. velocity of a particle $\nu_p \geq c/n$). As the refractive index of silica optical fibre is ~1.5, the threshold speed required to generate Čerenkov is ~0.7 times the speed of light. This corresponds to electrons and protons with energies of ~0.2MeV and ~0.38GeV respectively. In LEO the average flux with energies greater then this is of order 10^4 for electrons and 10^0 for protons.

If one (or several) of these particles intersect an optical fibre and pass near the core, the generated light can couple to a guiding mode in the fibre. In the case of NanoSpec, a dense region of radiation could lead to an additional background signal in the spectrum, thereby decreasing the signal to noise ratio. This effect has been documented in medical physics studies where optical fibres used in dosimetry are exposed to therapeutic particle beams.[13,14]

2.1.1 Coupling of Čerenkov in optical fibres

Čerenkov photons are emitted at an angle θ with respect to the particles direction of travel, forming the characteristic cone depicted in Fig. 1. This angle is given as,

$$\cos\theta = 1/(\beta n). \tag{1}$$

where n is the refractive index of the material, and β is the fraction of speed of light the particle is travelling at. In Fig. 1b a high energy particle intersects an optical fibre feed with an angle α. If the intersection occurs at such that $\alpha \approx \theta$ the generated light can be guided by the fibre, thus contaminating the spectrum.

In order to quantify the effect of Čerenkov radiation on a signal in optical fibre Law *et al.*[15] calculated the fraction of a Čerenkov cone that would be trapped using a ray tracing model of fibre. The actual intensity of Čerenkov generated by a charged particle passing through an optical fibre is given by the product of the path of the particle through the fibre and the intensity of Čerenkov radiation generated per unit distance. Using the Law *et al.*, model a rough estimate of coupling that will occur in fibre used by NanoSpec suggests that of order 10-100 photons are coupled. So a single event will have likely have very little impact on NanoSpec's performance, however in regions such as the magnetic poles and the SAA the cumulative effect of many events in single exposure could result in a detectable signal.

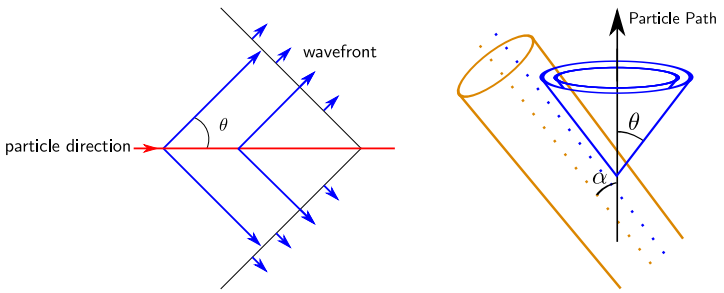

(a) (b)

Figure 1: *a)* A plane wavefront of Čerenkov radiation is formed at an angle θ to the velocity of the particle. *b)* Only the portion of the Čerenkov cone that intersects with the fibre core and is within in the critical angle of the fibre is trapped. Illustrated is the case where the cone is parallel to the fibre, which maximises the fraction of the cone trapped.[15]

3. DESIGN CONSIDERATIONS

The primary constraints, and thus design drivers for NanoSpec, can be split into 3 main factors. The first is the restricted area and volume of the satellite, and is perhaps the most stringent constraint. Fig. 2a is a diagram of the i-INPSIRE satellite showing the area that all the spacecraft systems and science payloads (including all optics, detectors/sensors and any additional control electronics of NanoSpec) must remain within this area. A side view of the design is shown in Fig. 2b, where the payload compartment, seen in the left side of the diagram, limits the cumulative height of the payload to 50 mm.

The overall cost of the spectrograph is the second major factor. The i-INSPIRE mission is a one way trip, so anything that is launched into orbit will not be recovered. In fact, given that we are scheduled on the first mission of IOS's N45 launch vehicle, there is a significant risk that the satellite will not achieve orbit. As a result we aim to keep the payload costs as low as possible, making use of commercially available parts and components where possible. Further, due to the low altitude and the actual mission time being fairly short (<4 weeks), we have neglected radiation hardness requirements in many of our components, opting for the industrial version where possible.

The third factor arises from the limited power available to the payload in orbit. As an isolated system in-orbit the power budget is strict, so the power requirements of detector used in the spectrograph are an important part of its design.

From these constraints we determined that the optimum design for the spectrograph would operate in the visible (~400-750nm). This is in due in part to the availability and performance of 'off the shelf' achromatic lenses and further supported by the wide availability of silicon CCD and CMOS detectors thanks to mass commercialisation of the technology.

4. OPTICAL DESIGN

4.1 Input Slit

NanoSpec is designed to be compatible with a photonic lantern input, however it has not yet been determined if the final flight instrument will utilise one (the current generation of lanterns are to large). The alternative is to form a pseudo-slit in NanoSpec with 8 independent SMFs. They are arranged in pairs, pointing out the ends and sides of the satellite, as illustrated by the red and blue lines in Fig. 2b. This initial arrangement is intended to maximise the chances that for any given orientation of the satellite, diffuse light from the Earth, Sun, or Moon (or a combination of these) will be coupled into one or more of the fibre pairs to produce a spectra . The fibres have a NA of 0.1 corresponding to a circular area with a radius of 40km when the fibre is aimed at the earth surface in orbit. Additionally, the fibre pairs consist of two different types of fibre in order to contrast their performance in the LEO environment.

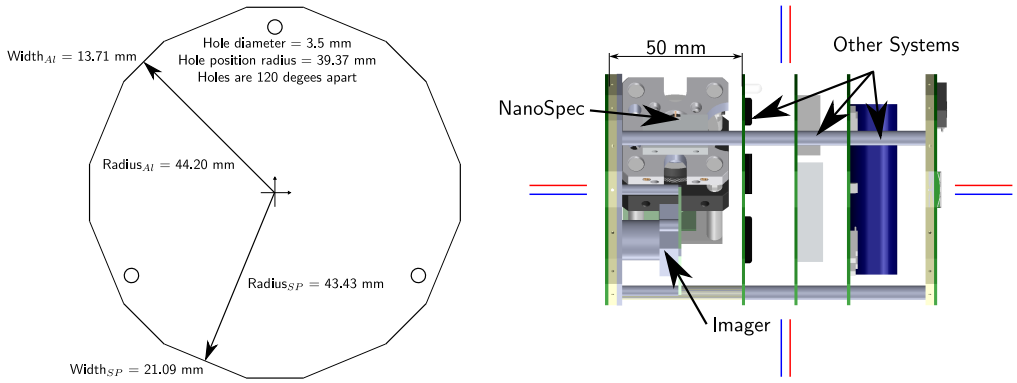

(a) (b)

Figure 2: *a)* Diagram showing the dimensions of top view of the i-INSPRE satellite. The NanoSpec housing must fit within this area to be compatible with the satellite design. *b)* Side view schematic of the satellite. The payloads, including NanoSpec, are located in the leftmost compartment, with the other satellite systems composing the remaining space.

The 8 SMFs are set in a v-groove fibre array manufactured by OzOptics[a]. The v-groove allows for the fibre inputs of the spectrograph to be precisely aligned and held. The fibre cores are separated by $127\mu m$, while the faces of the fibres share the same plane. The output face of the v-groove is the input of the spectrograph in place of a slit. The array of fibres are arranged parallel to the axis of the diffraction grating such that their dispersed images form 8 independent spectra.

The fibre pairs are composed of a typical step index fibre where light guiding is achieved via a higher refractive index in the core of the fibre then the cladding. While the second is a photonic crystal fibre (PCF) where light is guided by a pattern of air filled holes in the core of silica fibre. To our knowledge this will be the first time PCF has been demonstrated in a space environment. If NanoSpec does suffer from signal to noise ratio degradation due to Čerenkov light, we expect the PCF fibre spectra to exhibit better performance.This is because the PCF has less high-index material for the charged particle to pass through, and will thus generate less Čerenkov light.

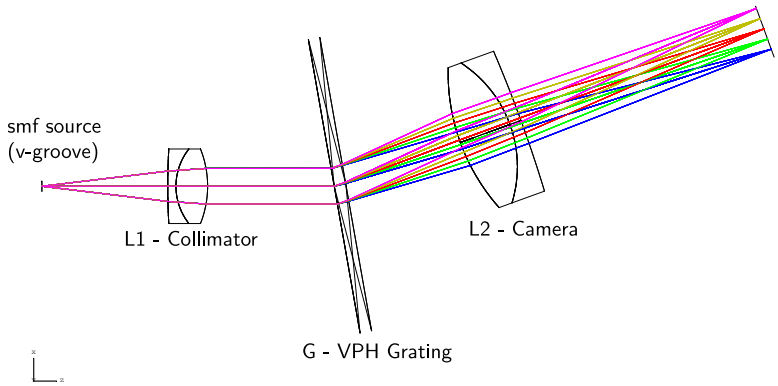

Figure 3: NanoSpec Optical Layout - Diagram of the current layout for the NanoSpec micro-spectrograph. The v-groove array of input fibres are stacked perpendicular the page. Wavelengths are evenly spaced from 450 to 700 nm.

4.2 Collimator and Camera Optics

The collimator must convert the Gaussian output beam of a SMFs to a collimated beam with out introducing any significant aberration. Further, it must do so without significant truncation of the Gaussian beam. Any truncation leads to a broadening of the focal PSF. Previous work indicates that the beams $1/e^2$ width should be $\leq 1/2$ (ideally 1/3) the diameter of the aperturing lens.[16–19] Here the limited factor is the magnification required to sampled the PSF correctly and the area the design is bound by in the satellite. The slight fold introduced by the grating slightly increases the maximum total length of the combined lens focal lengths.

The collimating system in NanoSpec is composed of carefully selected 'off the shelf' achromatic doublet lenses manufactured by the Newport Corporation[b] and Thorlabs[c]. The lenses are chosen such that they will create the largest collimate beam (as the beam size is directly proportion to the resolution) and remain diffraction limited, yet fit within the size constraints discussed previously. All lenses are anti-reflective coated for visible light (400-700nm).

Currently there are two versions of the collimator to suit two different detector pixel pitches ($2.2\mu m$ and $6\mu m$). The first is a single doublet with an effective focal length (EFL) of 12.7mm and a diameter of 6.5 mm, resulting is a Gaussian beam approximately 2 mm in diameter. The second version adds an additional doublet (with an 7mm EFL and diameter of 5mm) 1mm in front of the the first lens. This reduces the EFL of the collimator to 5.7mm and the collimated beam to 0.9mm. The reduced beam size in this case will also reduce the resolution of the spectrograph. In both cases the camera lens is a doublet with an EFL of 25.4mm and a diameter of 12.7 mm. In all instances the optics are essentially very close to diffraction limited in the visible, and have Gaussian truncation ratio better then required (less then then 1/3).

[a] http://www.ozoptics.com/
[b] http://www.newport.com
[c] http://www.thorlabs.com/

4.3 Grating

The dispersing element in the spectrograph is a volume phase holographic (VPH) grating manufactured by Wasatch Photonics[d]. A VPH consists of a dichromate gelatine substrate between two pieces of protective glass with an anti-reflective coating. The VPH diffracts light via fringes of refractive index variations written in the gelatine substrate with a controlled thickness,[20] rather than the physical lines/rules found in traditional gratings. This results in a grating that is 'blazed' such that $> 80\%$ of the diffracted light is transmitted in the 1st diffraction order ($m = 1$) over an extended wavelength range at angles θ consistent with the standard diffraction equation, $2d \sin\theta = m\lambda$. Further, the VPH grating offers very low scatter (which simplifies the design, and reduces background noise) and low wavefront distortion (necessary for a diffraction limited system).

4.3.1 Resolving Power

In a spectrograph the number of combining beams generated at the diffraction grating gives a fundamental limit on the spectal resolution. This is often given simply as the number of lines on the grating that are illuminated by the collimated beam (N) and the diffraction order (m) as follows,

$$\mathrm{R} = \frac{\lambda}{\Delta\lambda} = \underbrace{mN}_{\text{uniform}} , \tag{2}$$

where $\Delta\lambda$ is the smallest spectral feature that can be resolved (here we use 1.119 times the FWHM, which provides the same contrast in the focal plane as the Rayleigh criterion[18]) and λ is the wavelength being measured. However, Eqn. 2 assumes uniform illumination of the grating lines, whereas the beam in NanoSpec is Gaussian in nature. It can be shown[18,19] that the resolution of a Gaussian illuminated grating is given as follows,

$$R = \underbrace{2.38 \tan\theta \frac{d}{\lambda}}_{\text{Gaussian}}, \tag{3}$$

where θ is the diffraction angle and d is the collimated beam width. At first glance it would appear that a Gaussian beam results in a higher resolution, however this is not the case as the diameter in Eqn. 3 is the $1/e^2$ width (i.e. a 1 mm Gaussian beam illuminates more grating lines than a 1mm uniform beam, albeit unevenly). Eqn. 3 predicts a maximum resolution of 1450 and 650 (at 576nm) for the 2mm beam and 0.9 mm beams produced by the collimator version respectively.

4.4 Detector

Their are two detectors options for use in NanoSpec, one for ground testing and observation and the second will be used in flight. The first is a 5MP (2552 x 1964) detector with $2.2\mu m$ pixels while the second is a smaller VGA (640x480) format sensor with $6\mu m$ pixels. The advantage of the VGA detector over the 5MP detector is a simpler TTL level serial interface and higher sensitivity, the former allowing easier integration with the satellite hardware. However, due to the increased pixel size the spectral resolution and wavelength range are necessarily reduced. The 5MP detector has a USB interface, and allows greater controller over pixel binning and exposure times, but currently requires the use of a PC. This will allow for a more detailed study of the NanoSpec design's optimal performance, using either collimator.

4.5 Preliminary performance

Fig. 4 is a spectrum from NanoSpec (using the $2.2\mu m$ detector) of the low-pressure gas discharge lines of mercury and argon generated by a Hg-1 calibration source manufactured by OceanOptics[e]. We have used this to calibrate the wavelength scale and probe the resolution of NanoSpec. The inset in Fig. 4 is an expanded view of the first order mercury (Hg-I) spectral lines at 576.96 and 579.06nm. From these we determined the resolution, where $\Delta\lambda$ is the 1.119 times FWHM of the line. Measurements of both lines result in a resolving power on the order of R~1400 ($\Delta\lambda = 0.4$nm). This is remarkably close to the theoretical resolution given by Eqn. 3 for these

[d] `http://wasatchphotonics.com/`
[e] `http://www.oceanoptics.com`

wavelengths (~1450). Note, that when the $6\mu m$ detector is used, we expect the resolution to be roughly half (due to the decreased beam size).

This is extremely promising as it demonstrates that the device is very close to being diffraction-limited. Finally, initial measurements indicate that the throughput of the spectrograph is ~70%, where the primary loss of light is in other diffraction orders of the VPH (measure as the amount of light from the output of the fibre pseudo-slit that lands on the detector).

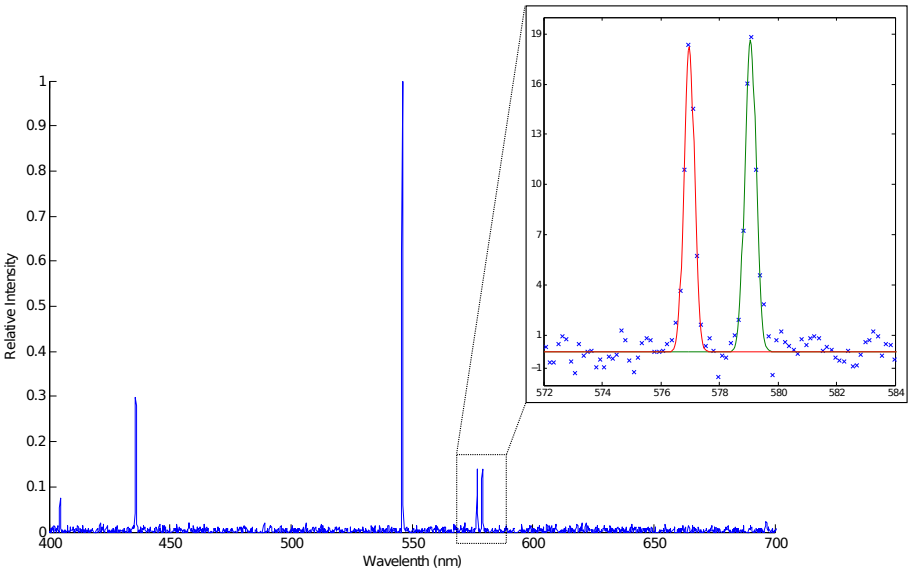

Figure 4: Example spectrum from NanoSpec of low-pressure gas discharge lines of mercury and argon captured using the $2.2\mu m$ pixel detector. Inset: Zoom in of the spectral lines at 576.96 and 579.06nm fitted with Gaussian profiles to determine the FWHM.

5. FUTURE PLANS

In late 2012 we plan to launch the i-INPSIRE satellite (including NanoSpec) on a high altitude weather ballon in preparation for space launch. Currently the anticipated space launch date is early 2013. Further preparation is underway, with plans for radiation testing, thermal vacuum testing and vibration bench analysis.

The next step beyond i-INSPIRE will likely be a larger payload on a balloon-based platform. A balloon-based instrument will allow us to use scientific grade detectors (which have a larger footprint) to construct a more sensitive NanoSpec. Paralleling that, we hope to move toward a fully photonic device, likely using an arrayed waveguide grating. The first steps towards such a device has been demonstrated by Cvetojevic *et al.*[21,22] However, these devices are currently limited to telecom IR wavelengths, where detector technology is not as compact as in the visible.

6. CONCLUSION

Here we have presented a brief review of Nanospec, a diffraction-limited micro-spectrograph for the i-INSPIRE pico-satellite at the University of Sydney. Its design harnesses a pseudo-slit composed of SMFs, allowing diffraction limited performance. The design is composed of purely 'off the shelf' components and is compact enough to fit within the confine of the i-INSPIRE satellite. We have demonstrated that it has a resolving power of 1400 (~0.4nm) at ~578nm, remarkably close to the 1450 theoretical limit. With NanoSpec we intend to demonstrate diffraction limited spectrograph in space and study the effects of the LEO radiation environment on such device in early 2013.

REFERENCES

[1] Bland-Hawthorn, J. et al., "PIMMS: photonic integrated multimode microspectrograph," in [*Ground-based and Airborne Instrumentation for Astronomy III*], McLean, I. S., Ramsay, S. K., and Takami, H., eds., *Proc. SPIE* **7735**, 77350N (2010).

[2] Leon-Saval, S. G., Birks, T. A., Bland-Hawthorn, J., and Englund, M., "Multimode fiber devices with single-mode performance," *Optics Letters* **30**, 2545–2547 (2005).

[3] Noordegraaf, D., Skovgaard, P. M., Nielsen, M. D., and Bland-Hawthorn, J., "Efficient multi-mode to single-mode coupling in a photonic lantern," *Optics Express* **17**, 1988–1994 (2009).

[4] Leon-Saval, S. G., Argyros, A., and Bland-Hawthorn, J., "Photonic lanterns: a study of light propagation in multimode to single-mode converters," *Optics Express* **18**, 8430–8439 (2010).

[5] Fogarty, L. M. R. et al., "The i-INSPIRE Satellite," in [*Space Telescopes and Instrumentation 2012: Optical, Infrared, and Millimeter Wave*], *Proc. SPIE* **8442**, 844244 (2012).

[6] Fogarty, L. et al., "The initial-INtegrated SPectrograph, Imager and Radiation Explorer (i-INSPIRE) - a university satellite project.," in [*Proceeding of the 11th Australian Space Science Conference*], (2011).

[7] Xiao, S. et al., "i-INSPIRE Tube-Satellite Bus Design," in [*Proceeding of the 11th Australian Space Science Conference*], (2011).

[8] Betters, C. et al., "Instrumentation of the i-INSPIRE satellite.," in [*Proceeding of the 11th Australian Space Science Conference*], (2011).

[9] Badhwar, G. D., "The radiation environment in low-Earth orbit," *Radiation research* **148**, S3–S10 (1997).

[10] Heynderickx, D., Quaghebeur, B., Wera, J., Daly, E. J., and Evans, H. D. R., "New radiation environment and effects models in the European Space Agency's Space Environment Information System (SPENVIS)," *Space Weather* **2**(10), S10S03 (2004).

[11] Abraham, J. et al., "Properties and performance of the prototype instrument for the pierre auger observatory," *Nuclear Instruments and Methods in Physics Research Section A: Accelerators, Spectrometers, Detectors and Associated Equipment* **523**, 50–95 (2004).

[12] Fukuda, Y. et al., "Measurement of a small atmospheric ν_μ/ν_e ratio," *Physics Letters B* **433**, 9–18 (1998).

[13] Lambert, J., Yin, Y., McKenzie, D. R., Law, S., and Suchowerska, N., "Cerenkov light spectrum in an optical fiber exposed to a photon or electron radiation therapy beam," *Applied Optics* **48**(18), 3362–3367 (2009).

[14] Law, S. H., Suchowerska, N., McKenzie, D. R., Fleming, S. C., and Lin, T., "Transmission of Čerenkov radiation in optical fibers," *Optics Letters* **32**(10), 1205–1207 (2007).

[15] Law, S. H., Fleming, S. C., Suchowerska, N., and McKenzie, D. R., "Optical fiber design and the trapping of Cerenkov radiation," *Applied Optics* **45**(36), 9151–9159 (2006).

[16] Belland, P. and Crenn, J. P., "Changes in the characteristics of a gaussian beam weakly diffracted by a circular aperture," *Applied Optics* **21**(3), 522–527 (1982).

[17] Mahajan, V., [*Optical Imaging and Aberrations: Wave diffraction optics*], SPIE Optical Engineering Press, 337-366 (2001).

[18] Robertson, G. and Bland-Hawthorn, J., "Compact high-resolution spectrographs for large and extremely large telescopes: using the diffraction limit," in [*Ground-based and Airborne Instrumentation for Astronomy IV*], *Proc. SPIE* **8446**, 844674 (2012).

[19] Betters, C. H. et al., "Demonstration and design of a compact diffraction limited spectrograph.," in [*Ground-based and Airborne Instrumentation for Astronomy IV*], *Proc. SPIE* **8446**, 8446129 (2012).

[20] Barden, S. C., Arns, J. A., Colburn, W. S., and Williams, J. B., "VolumePhase Holographic Gratings and the Efficiency of Three Simple VolumePhase Holographic Gratings," *Publications of the Astronomical Society of the Pacific* **112**(772), 809–820 (2000).

[21] Cvetojevic, N., Lawrence, J. S., Ellis, S. C., Bland-Hawthorn, J., Haynes, R., and Horton, A., "Characterization and on-sky demonstration of an integrated photonic spectrograph for astronomy," *Optics Express* **17**(21), 18643–18650 (2009).

[22] Cvetojevic, N., Jovanovic, N., Lawrence, J., Withford, M., and Bland-Hawthorn, J., "Developing arrayed waveguide grating spectrographs for multi-object astronomical spectroscopy," *Optics Express* **20**(3), 2062–2072 (2012).